N73-25823
NASA TM X-2811

NASA TECHNICAL MEMORANDUM

NASA TM X-2811

EXPERIMENTAL COLD-FLOW EVALUATION OF A RAM-AIR-COOLED PLUG-NOZZLE CONCEPT FOR AFTERBURNING TURBOJET ENGINES

by David M. Straight, Douglas E. Harrington, and Stanley M. Nosek

Lewis Research Center
Cleveland, Ohio 44135

NATIONAL AERONAUTICS AND SPACE ADMINISTRATION • WASHINGTON, D. C. • JUNE 1973

1. Report No.	2. Government Accession No.	3. Recipient's Catalog No.
NASA TM X-2811		

4. Title and Subtitle	5. Report Date
EXPERIMENTAL COLD-FLOW EVALUATION OF A RAM-AIR-COOLED PLUG-NOZZLE CONCEPT FOR AFTERBURNING TURBOJET ENGINES	June 1973
	6. Performing Organization Code

7. Author(s)	8. Performing Organization Report No.
David M. Straight, Douglas E. Harrington, and Stanley M. Nosek	E-7387
	10. Work Unit No. 501-24

9. Performing Organization Name and Address	11. Contract or Grant No.
Lewis Research Center National Aeronautics and Space Administration Cleveland, Ohio 44135	
	13. Type of Report and Period Covered
12. Sponsoring Agency Name and Address	Technical Memorandum
National Aeronautics and Space Administration Washington, D.C. 20546	14. Sponsoring Agency Code

15. Supplementary Notes

16. Abstract

A new concept for plug nozzles cooled by inlet ram air is presented. Experimental data obtained with a small scale model, 21.59-cm (8.5-in.) diameter, in a static altitude facility demonstrated high thrust performance and excellent pumping characteristics. Tests were made at nozzle pressure ratios simulating supersonic cruise and takeoff conditions. Effect of plug size, outer shroud length, and varying amounts of secondary flow were investigated.

17. Key Words (Suggested by Author(s))	18. Distribution Statement
Nozzles; Plug nozzles; Exhaust nozzles; Nozzle design; Nozzle geometry; Nozzle performance; Plug nozzle cooling	Unclassified - unlimited

19. Security Classif. (of this report)	20. Security Classif. (of this page)	21. No. of Pages	22. Price*
Unclassified	Unclassified	25	$3.00

* For sale by the National Technical Information Service, Springfield, Virginia 22151

EXPERIMENTAL COLD-FLOW EVALUATION OF A RAM-AIR-COOLED PLUG-NOZZLE CONCEPT FOR AFTERBURNING TURBOJET ENGINES

by David M. Straight, Douglas E. Harrington, and Stanley M. Nosek

Lewis Research Center

SUMMARY

The thrust and pumping characteristics of a ram-air-cooled plug-nozzle concept were obtained with an 21.59-centimeter (8.5-in.) diameter model. Preliminary data obtained in a static cold-flow altitude facility indicated nozzle thrust efficiencies near 100 percent at simulated supersonic cruise pressure ratios. An efficiency of 98.5 percent was obtained at a pressure ratio of 4.0 corresponding to a climb condition near sea level takeoff.

Sufficient quantities of ram air were pumped by the primary jet expanding along the plug surface to meet calculated plug cooling air requirements for an afterburning engine at static conditions.

Data are also presented on the effect of plug size, outer shroud length, and varying amounts of secondary flow on thrust and pumping.

INTRODUCTION

The plug nozzle is an attractive concept for application to supersonic cruise aircraft. In particular, low angle conical plug nozzles have demonstrated efficient operation over a wide range of operating conditions (refs. 1 to 6). But one of the design problems encountered in maintaining high performance over the range of flight conditions is that of cooling the plug that is immersed in the hot gas stream. A number of cooling schemes applicable to turbojet exhaust nozzles are reported in references 7 to 9. Of the various schemes proposed, film cooling with air is most commonly used. Results of various film cooling investigations on plug nozzles are reported in references 10 to 12.

The purpose of this report is to present preliminary test data on a new plug nozzle concept. A limited number of model configurations were tested to determine if further investigation is warranted. The plug-nozzle concept investigated is film cooled using external or engine inlet ram air which should have a lower net thrust penalty than if compressor bleed air were used. The cooling concept differs from other film-cooled plugs in that the relatively low energy ram air from the inlet is directed down the plug through a relatively large slot that allows the primary stream to pump adequate ambient air for cooling during static operations.

Three configurations of a 21.59-centimeter (8.5-in.) diameter model of the nozzle were tested in a cold-flow static altitude test facility at the Lewis Research Center to obtain thrust and pumping characteristics. The configurations were chosen to determine performance at two of the more important operating conditions; supersonic cruise and sea-level takeoff. Two configurations, with two plug sizes, were run at the supersonic cruise condition (high nozzle pressure ratios and extended outer shroud) to determine the effect of the variation of the large film cooling slot on thrust performance. One configuration, with the larger plug, was run at the sea-level takeoff condition (low pressure ratio and retracted outer shroud) to determine if cooling air could be pumped with zero ram pressure.

RAM AIR COOLED PLUG NOZZLE CONCEPT

A conceptual sketch of the ram-air-cooled plug nozzle on a large afterburning turbojet engine is presented in figure 1. Part of the inlet ram air flow is ducted through crossover struts upstream of the afterburner and then through the plug support sting to a large film cooling annulus on the plug wall a short distance downstream of the primary nozzle throat. The translating outer shroud and the fixed position outer primary shroud are cylindrical to reduce or eliminate boattail drag.

The primary nozzle throat area variation required for afterburning operation would be provided by varying the position of an inner primary shroud. Previous plug-nozzle configurations generally achieved area variation using a movable outer primary shroud. Mechanically, the position of the inner primary shroud could be obtained by using an overlapping leaf type of construction. The plug size is large enough to conveniently provide a relatively cool space for the storage of actuators and umbrella type of thrust reverser mechanisms.

A brief study of applying the ram-air-cooled plug-nozzle concept to a duct burning turbofan engine indicated that the concept may also be applicable to other turbine engine cycles. Either ram air or fan-discharge air could be used for cooling the plug in turbofan engines.

APPARATUS AND PROCEDURE

Installation

A schematic of the nozzle installed in the static test facility is shown in figure 2. The nozzle was attached by an adapter to a section of pipe rigidly mounted on a bedplate. The bedplate was freely suspended by four flexure rods. The metric portion of the installation (bedplate, adapter, nozzle, etc.) was separated from the grounded section by means of a flexible bellows. Thus, the metric portion was free to move fore and aft. Both external and internal pressure forces acting on the metric section were measured with a load cell mounted between the bedplate and a grounded portion of the facility. Nozzle gross thrust was then determined from the load cell measurement, primary inlet momentum, and several facility tare forces.

Facility Calibration

Nozzle primary weight flow was calculated from pressure and temperature measurements at the primary air metering station and a flow coefficient that had been determined with an ASME calibration nozzle. Inner and outer secondary weight flows were measured with standard ASME flow metering orifices located in external supply lines.

The ASME nozzle was also used to calibrate the thrust of the metric portion of the installation. This was done before and after testing the ram-air-cooled plug nozzle. The data of more than 250 points that were generated in these calibrations are presented in figure 3. The gross thrust coefficients calculated from the measured thrusts are plotted as a function of the nozzle pressure ratio and compared with the theoretical values. Practically all of the points fall within ±0.5 percent of deviation from the theoretical. The standard deviation is 0.0024. It must be noted, however, that the results with the calibration nozzle does not include the effect of bringing secondary air onto the metric section. The bourdon tube effect of the flexible secondary air lines induced some small additional thrust. Thus, the efficiencies of the ram-air-cooled plug, in some cases, go over 100 percent. Although this error is probably small, it is significant enough to recognize in evaluating the results with the plug nozzle.

Nozzle Configurations

The three basic nozzle configurations that were tested are shown in figure 4. Pertinent area ratios are listed in table I. Variation of inner secondary flow area A_{is} was simulated by using two different sizes of plugs. (Symbols are defined in appendix A.) The small plug was tested with the outer shroud completely extended ($X/D_m = 0.82$) to its supersonic cruise position. The large plug was tested with both extended ($X/D_m = 0.82$) and retracted ($X/D_m = -0.16$) shrouds. The retracted outer shroud corresponds to takeoff position. The geometric details of the flow passages are shown in figure 5. The radius of curvature of the inner primary shroud was designed to be relatively large to minimize flow distortion at the primary nozzle throat. In addition, a small amount of internal expansion was provided for the primary flow. Photographs of the nozzle are presented in figure 6, which shows the major components of the ram-air-cooled plug nozzle.

TABLE I. - AREA RATIOS IN NOZZLE CONFIGURATIONS

[$A_8/A_m = 0.266$; $A_{lip}/A_g = 1.13$]

Nozzle configuration	Area ratios			
	A_{pL}/A_m	A_{is}/A_m	A_{os}/A_m	A_9/A_8
Large plug, extended shroud	0.375	0.138	0.145	3.27
Large plug, retracted shroud	.375	.138	.145	----
Small plug, extended shroud	.205	.309	.145	3.57

Model Instrumentation

Figure 7 presents the instrumentation that was used on the model. The instrumentation at station 7 (fig. 7(a)) was used primarily to determine the flow properties of the various streams as they entered the nozzle. All total-pressure rakes were equal area weighted and the static-pressure orifices were offset from the rakes to minimize disturbances from these rakes. The static-pressure orifices for determining component forces are shown in figure 7(b). All of these pressures (except those on the outer shroud) were measured at the centroids of equal axially projected areas. The component forces were then determined by summing the pressures and multiplying by the total

axially projected area of the desired surface. Orifices 3 to 6 were not used in the results presented here.

Procedure

Nozzle pressure ratios were set by maintaining a constant nozzle inlet pressure $P_{t,7}$ and varying the tank pressure P_0 with the exhausters. Each of the nozzle configurations was tested over a range of pressure ratios encompassing the design conditions. At design conditions, the inner secondary weight flow ratio $\omega_{is}\sqrt{\tau_{is}}$ was varied from 0 to 8 percent and the outer weight flow ratio $\omega_{os}\sqrt{\tau_{os}}$ was varied from 0 to 6 percent.

Thrust Calculations

The ideal jet thrust for each of the primary and secondary flows was calculated from the measured mass flow rate expanded from its measured total pressure to tank static pressure P_0. Nozzle efficiency is then defined as the ratio of the gross thrust to the sum of the ideal thrusts of both the primary and secondary flows:

$$\text{Nozzle efficiency} = \frac{F_m}{F_i} \quad \text{or} \quad \frac{F_c}{F_i}$$

In addition, the measured nozzle gross thrust coefficient was also calculated. It is defined as the ratio of the measured gross thrust to the ideal thrust of the primary flow:

$$\text{Nozzle gross thrust coefficient} = \frac{F_m}{F_{ip}}$$

RESULTS AND DISCUSSION

Thrust From Load Cell Measurements

The cold-flow thrust performance of the three nozzle configurations tested is shown in figure 8. Between nozzle pressure ratios of 22 and 30, the nozzle efficiency based on measured thrust data shows values near 100 percent for the large plug, extended

shroud configuration. (See Facility Calibration section.) Below a pressure ratio of 22, the nozzle efficiency decreases because the internal area ratio with the long shroud is too large for these lower pressure ratios.

The data obtained with the outer shroud in a simulated retracted position (large plug) showed a peak efficiency of 0.985 occurring at a pressure ratio of 4.0, slightly higher than the sea level takeoff design pressure ratio of 3.3. The actual effective internal area ratio was apparently slightly larger than the design value.

The performance of the nozzle at intermediate pressure ratios from 5 to 15 (corresponding to subsonic cruise and acceleration) should improve if intermediate shroud lengths were used.

The small plug model was run (with the extended shroud) to determine the thrust losses that would occur if a larger plug cooling air slot height (inner secondary area, A_{is}) was needed to adequately cool the plug during afterburner operation on an engine.

The results in figure 8 show that the thrust was only 0.5 to 1.0 percent lower over the complete range of pressure ratios, even though the slot area was increased from 14 to 31 percent of the projected area of the nozzle.

All data in figure 8 were obtained at constant design corrected secondary weight flow ratios of 0.05 for the inner secondary and 0.03 for the outer secondary. All three configurations, however, were run over a wide range of inner and outer corrected secondary flows to determine the sensitivity of the design concept to operation at off-design flow rates. The effect of secondary flow on nozzle efficiency is presented in figure 9. With the extended shroud, there was little change in nozzle efficiency for changes in corrected secondary weight flow ratios from 0.02 to 0.08 for both inner and outer secondaries at a nozzle pressure ratio of 28. When the secondary flows were reduced to zero, however, there was about a 1.5 percent loss in efficiency. In the retracted shroud configuration, increase in inner secondary flow increased efficiency, and increased outer secondary flow slightly reduced efficiency at a nozzle pressure ratio of 3.

The gross thrust coefficients are shown in figures 10 and 11. Figure 10 presents the variation with pressure ratio, and figure 11 presents the variation with inner (fig. 11(a)) and outer (fig. 11(b)) corrected secondary weight flow ratios.

Thrust From Component Pressure Forces

A further indication of the high performance levels (figs. 8 to 11) could be obtained from the many surface-pressure measurements described in the instrumentation section. Total thrust was determined by summing the stream momentums and pressure forces on all the nozzle components. (Drag from the plug support struts was not included.) Calculations were on a one-dimensional flow basis with no friction.

Typical summary curves resulting from component force analyses are shown in figure 12 where the small plug configuration is compared with the large plug configuration. The largest difference between the two configurations occurs in the surface force on the aft end of the plug (fig. 12(a)), where, as expected, the large plug has a force nearly twice that of the small plug at the design pressure ratio of 28. To offset some of this difference, however, the inner secondary of the small plug configuration has a higher force than the large plug inner secondary ($P_{t,7}/P_0 = 28$ in fig. 12(b)). The net result was that overall thrust performance with the small plug was less than 0.5 percent lower than for the large plug (see fig. 8). The outer secondary (fig. 12(c)) and primary (fig. 12(d)) component forces are nearly the same for both plug sizes. The sum of all the component forces presented in figure 12(e) show about the same difference between the performance with the two plug sizes as the measured thrust data presented in figure 8.

A direct comparison of the nozzle efficiencies obtained by component forces with that obtained from load cell measurements is shown in figure 13 for the three configurations tested. The component method shows higher performance than the load cell method although the shape of the curves are nearly identical. No corrections for friction forces were made in the component force data in figure 13. However, an estimate of the friction force was made at the design pressure ratio of 28, using two different boundary layer methods (refs. 13 and 14). Both methods reduced the efficiency by about 1/2 percentage point. Thus both load cell measurements and component analyses results show that the performance of the nozzle is high.

Pumping Characteristics

The pumping characteristics of the inner secondary flow passage for the three configurations tested are shown in figure 14. All three show low secondary passage pressures over a range of primary nozzle pressure ratios and secondary air flow rates. The primary airstream of the small plug configuration pumps the secondary to lower pressures than the large plug because the secondary to primary area ratio is larger. Note that the primary air stream of the large plug configurations pumps secondary air ($\omega_{is}\sqrt{\tau_{is}} = 0.05$) to the same pressure level ($P_{t,is}/P_{t,7} = 0.2$) with the outer shroud in both retracted (fig. 14(c)) and extended (fig. 14(b)) positions.

Heat-transfer calculations were made for a ram-air-cooled plug nozzle installed on a typical small 63.5-centimeter (25-in.) outer shroud diameter, afterburning turbojet engine. The results of the plug cooling calculations are shown in figure 15. An inner secondary corrected airflow of 4 percent was predicted to be adequate to keep the maximum plug wall temperature within safe operating limits at sea level takeoff conditions.

Pumping data were obtained with the model at a pressure ratio near that required at sea level takeoff conditions ($P_{t,7}/P_0 = 3.0$) to determine if the pumping characteristics of the ram-air cooled-plug nozzle could provide the amount of air required for cooling the plug (fig. 15). The data are presented in figure 16 as a function of corrected inner secondary flow rate ratio. The data show that a corrected inner secondary flow ratio of 5 percent is pumped at this zero ram condition with 5 percent of ambient pressure still available for duct flow losses through the secondary air passages ($P_{t,is}/P_0 = 0.95$). This pumping occurs by the primary jet expanding along the plug surface even with the outer shroud in the retracted position.

The pumping characteristics of the outer secondary flow passage are presented in figure 17. Comparison of figure 17 with figure 14 shows that with the large plug and extended shroud the outer secondary pressures are pumped to lower levels than the inner secondary at corresponding corrected flow rates.

SUMMARY OF RESULTS

The thrust and pumping characteristics of a ram-air-cooled plug-nozzle concept were obtained by testing a 21.59-centimeter (8.5-in.) diameter model in a static cold-flow altitude test facility. The general results were as follows:

1. Nozzle thrust efficiencies were near 100 percent at the supersonic cruise design nozzle pressure ratio of 28. The thrust efficiency was 98.5 percent at a pressure ratio of 4.0 corresponding to a climb condition near sea level. These high efficiency levels were confirmed by component force analyses.

2. Sufficient quantities of low pressure (ram) air were pumped by the primary jet expanding along the plug surface to meet calculated film cooling air requirements for a plug nozzle operation on an afterburning engine at sea level takeoff conditions. Expansion along the plug surface created adequate pumping with the outer shroud in a retracted position. (Corrected inner secondary weight flow ratio of 5 percent at an inner secondary to ambient pressure ratio of 0.95.)

3. The loss in aft-end plug force that resulted when the plug size was reduced was partly compensated for by an increase in force along the inner secondary (plug cooling air) flow passage, with the net result that overall thrust performance with the small plug was less than 0.5 percent lower than for the large plug at a nozzle pressure ratio of 28.

CONCLUDING REMARKS

The results from the limited number of configurations tested show that the ram-air-

cooled plug-nozzle concept has the potential of high thrust performance with low performance penalty due to cooling airflows. In addition, the nozzle concept has good pumping characteristics with low thrust loss penalty at the design points investigated.

The favorable results obtained indicate that further investigation is desirable. Some of the variables of interest are intermediate shroud lengths (for transonic operating conditions), various primary throat areas (required for afterburning), external flow effects, and hot flow tests to determine minimum cooling air flow rates for various afterburning levels and external flow conditions. Also desirable are installation and mission analyses to assess the ram-drag penalty associated with providing the cooling air.

Lewis Research Center,
National Aeronautics and Space Administration,
Cleveland, Ohio, April 11, 1973,
501-24.

APPENDIX - SYMBOLS

A_{is} inner secondary flow area at primary lip

A_{os} outer secondary flow area

A_{lip} primary nozzle flow area in lip plane

A_8 primary nozzle throat area

A_9 flow area between end of extended outer shroud and plug surface

d_m model diameter

F_c total of all component forces (stream momentum and pressure forces)

F_i sum of ideal isentropic thrusts (primary and two secondaries)

F_{ip} ideal isentropic thrust of primary stream

F_{is} inner secondary component forces (stream momentum and pressure forces)

F_m measured gross thrust (based on load cell)

F_{os} outer secondary component forces (stream momentum and pressure forces)

F_p primary stream component forces (stream momentum and pressure forces from station 8 to lip plane)

F_{pl} aft plug surface pressure force

L length of plug from primary lip to aft end

P_0 altitude static pressure in test chamber

$P_{t,is}$ inner secondary total pressure at station 7

$P_{t,os}$ outer secondary total pressure at station 7

$P_{t,7}$ primary total pressure at station 7

T_{is} inner secondary air total temperature

T_{os} outer secondary air total temperature

T_p primary-air total temperature

W_{is} inner secondary airflow rate

W_{os} outer secondary airflow rate

W_p primary airflow rate

X axial distance from inner primary lip

$\omega_{is}\sqrt{\tau_{is}}$ corrected inner secondary flow ratio, $W_{is}/W_p\sqrt{T_{is}/T_p}$

$\omega_{os}\sqrt{\tau_{os}}$ corrected outer secondary flow ratio, $W_{os}/W_p\sqrt{T_{os}/T_p}$

REFERENCES

1. Bresnahan, Donald L.; and Johns, Albert L.: Cold Flow Investigation of a Low Angle Turbojet Plug Nozzle with Fixed Throat and Translating Shroud at Mach Numbers from 0 to 2.0. NASA TM X-1619, 1968.

2. Bresnahan, Donald L.: Experimental Investigation of a 10^{o} Conical Turbojet Plug Nozzle with Iris Primary and Translating Shroud at Mach Numbers from 0 to 2.0. NASA TM X-1709, 1968.

3. Bresnahan, Donald L.: Experimental Investigation of a 10^{o} Conical Turbojet Plug Nozzle with Translating Primary and Secondary Shrouds at Mach Numbers from 0 to 2.0. NASA TM X-1777, 1969.

4. Johns, Albert L.: Quiescent-Air Performance of a Truncated Turbojet Plug Nozzle with Shroud and Plug Base Flows from a Common Source. NASA TM X-1807, 1969.

5. Harrington, Douglas E.: Performance of Convergent and Plug Nozzles at Mach Numbers from 0 to 1.97. NASA TM X-2112, 1970.

6. Harrington, Douglas E.: Performance of a 10^{o} Conical Plug Nozzle with Various Primary Flap and Nacelle Configurations at Mach Numbers from 0 to 1.97. NASA TM X-2086, 1970.

7. Eckert, E. R. G.; and Livingood, John N. B.: Comparison of Effectiveness of Convection -, Transpiration -, and Film-Cooling Methods with Air as Coolant. NACA Rep. 1182, 1954.

8. Papell, S. Stephen; and Trout, Arthur M.: Experimental Investigation of Air Film Cooling Applied to an Adiabatic Wall by Means of an Axially Discharging Slot. NASA TN D-9, 1959.

9. Papell, S. Stephen: Effect of Gaseous Film Cooling of Coolant Injection Through Angled Slots and Normal Holes. NASA TN D-299, 1960.

10. Jeracki, Robert J.; and Chenoweth, Francis C.: Coolant Flow Effects on the Performance of a Conical Plug Nozzle at Mach Numbers from 0 to 2.0. NASA TM X-2076, 1970.

11. Chenoweth, Francis C.; and Lieberman, Arthur: Experimental Investigation of Heat-Transfer Characteristics of a Film-Cooled Plug Nozzle with Translating Shroud. NASA TN D-6160, 1971.

12. Clark, John S.; and Lieberman, Arthur: Thermal Design Study of an Air-Cooled Plug-Nozzle System for a Supersonic-Cruise Aircraft. NASA TM X-2475, 1972.

13. Elliot, David G.; Bartz, Donald R.; and Silver, Sidney: Calculation of Turbulent Boundary-Layer Growth and Heat Transfer in Axi-Symmetric Nozzles. Tech. Rep. 32-387, Jet Propulsion Lab., California Inst. Tech., Feb. 15, 1963.

14. Spalding, D. B.; and Patankar, S. V.: Heat and Mass Transfer in Boundary Layer. Morgan-Grampian Books, Ltd., 1967.

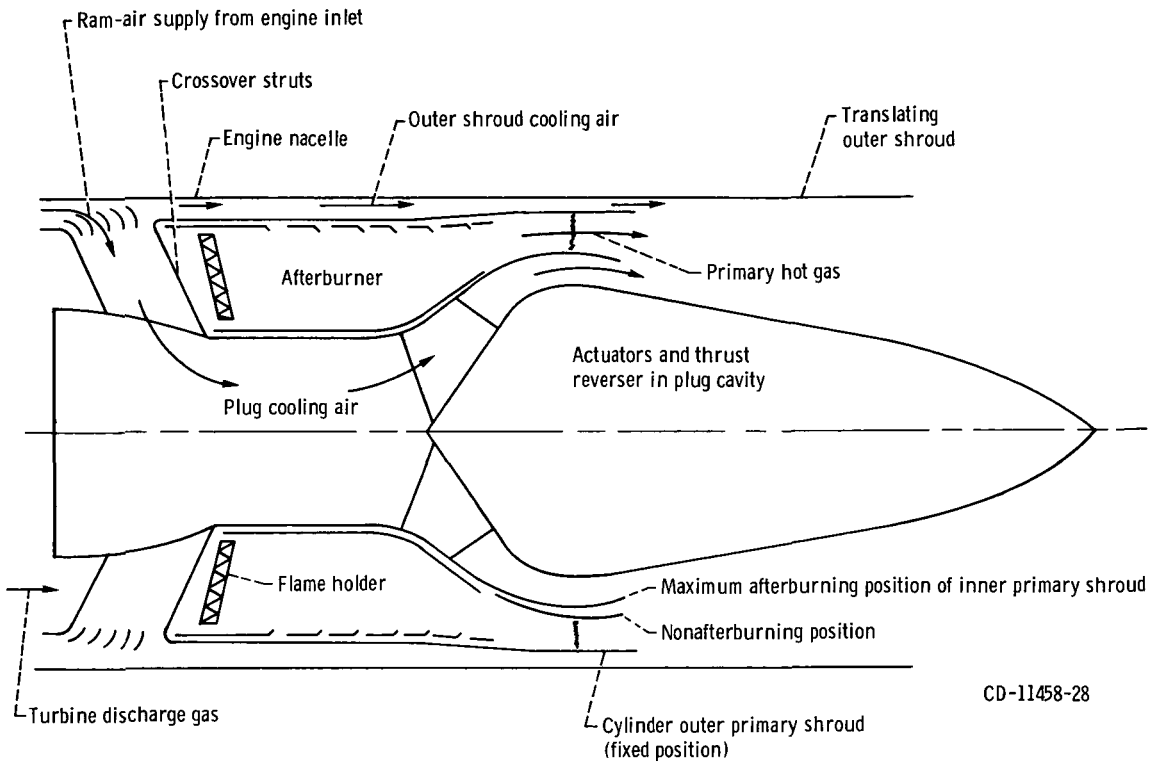

Figure 1. - Conceptual sketch of a ram-air-cooled plug nozzle for typical large afterburning turbojet engine.

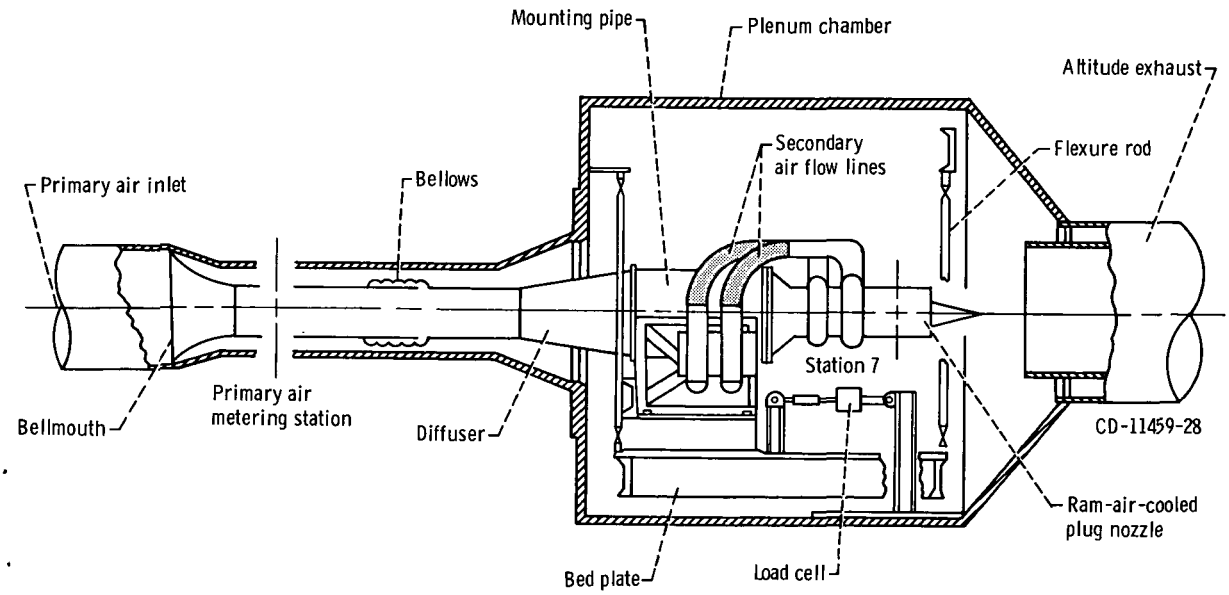

Figure 2. - Static test facility.

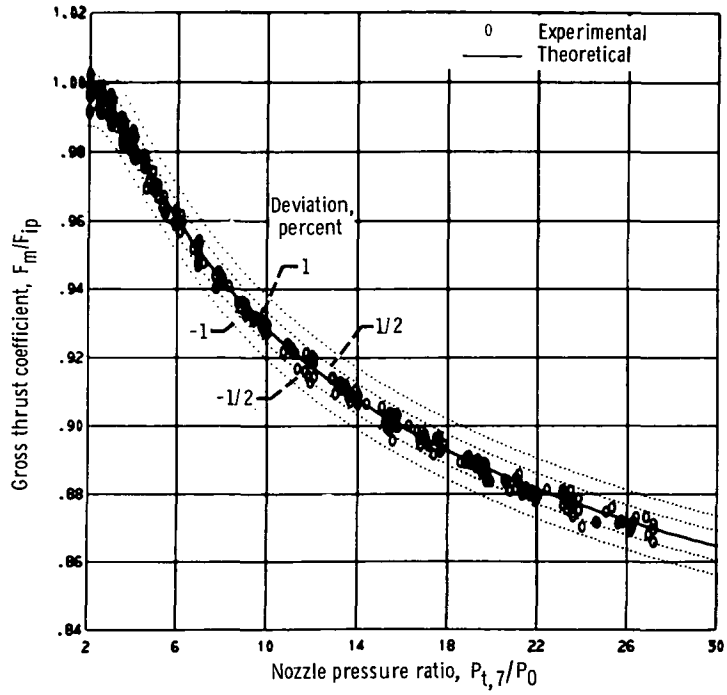

Figure 3. - Internal performance of ASME calibration nozzle. Standard deviation, 0.0024.

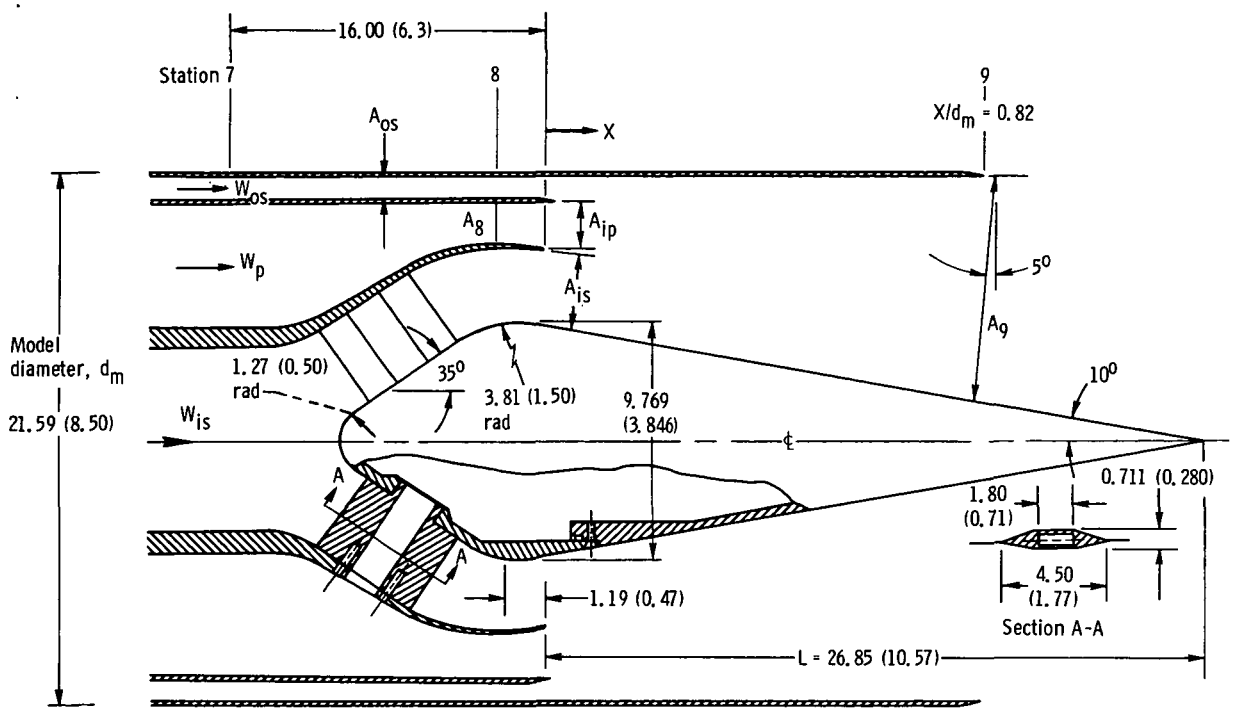

(a) Small plug with extended shroud ($X/d_m = 0.82$).

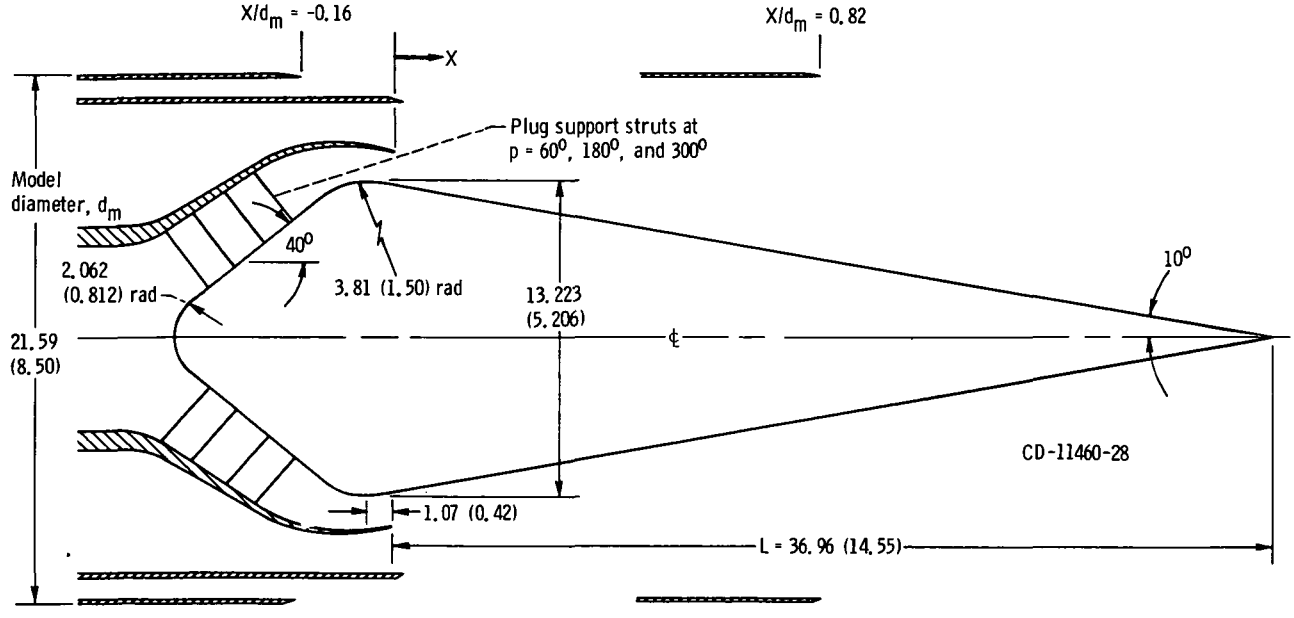

(b) Large plug with retracted shroud ($X/d_m = -0.16$) and extended shroud ($X/d_m = 0.82$).

Figure 4. - Geometric details of ram-air-cooled plug-nozzle model. (All dimensions are in cm (in.).)

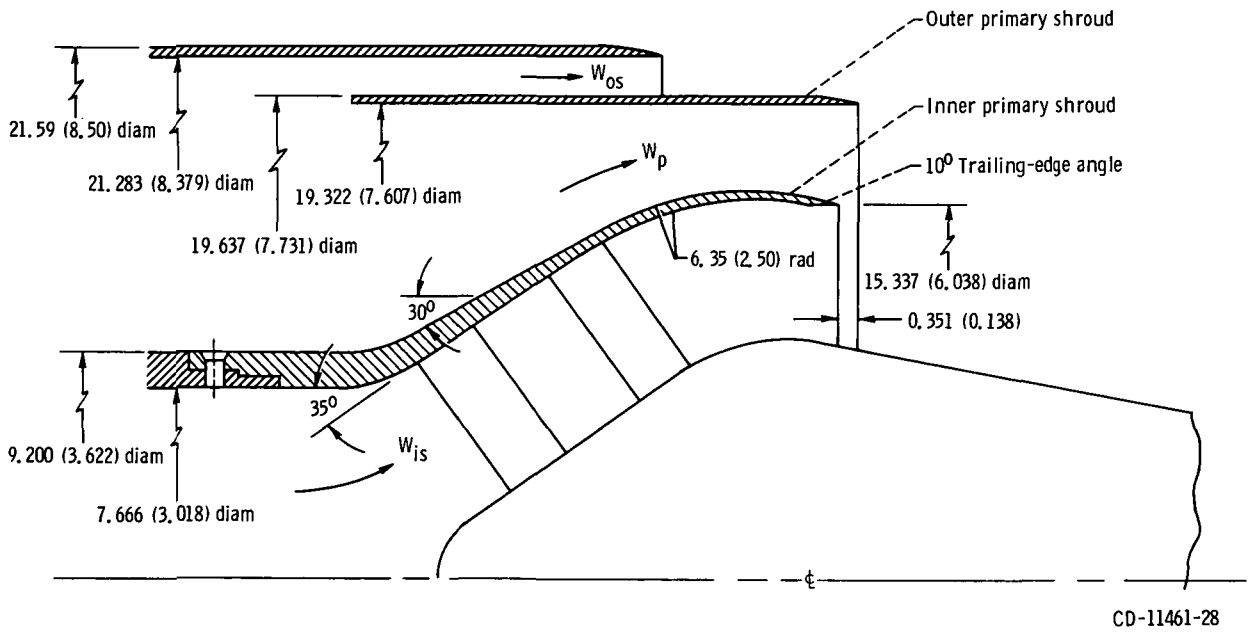

Figure 5. - Nozzle flow passage details. (All dimensions in cm (in.).)

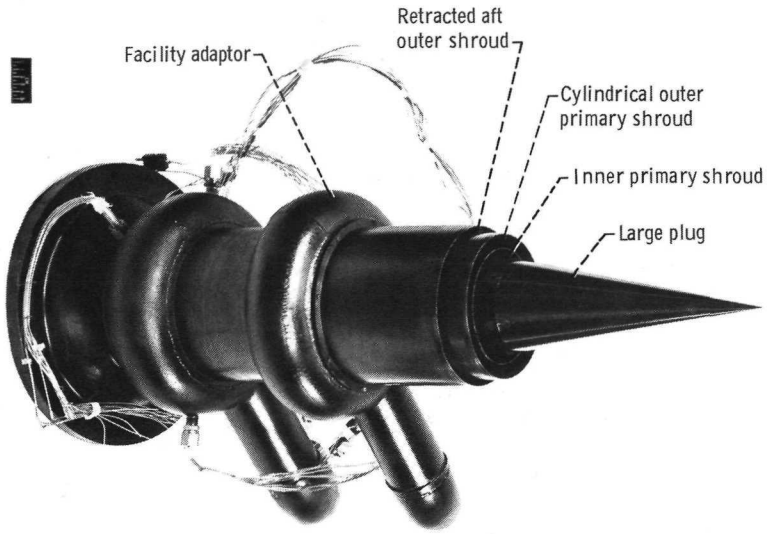

C-72-3298

(a) Large plug, retracted shroud.

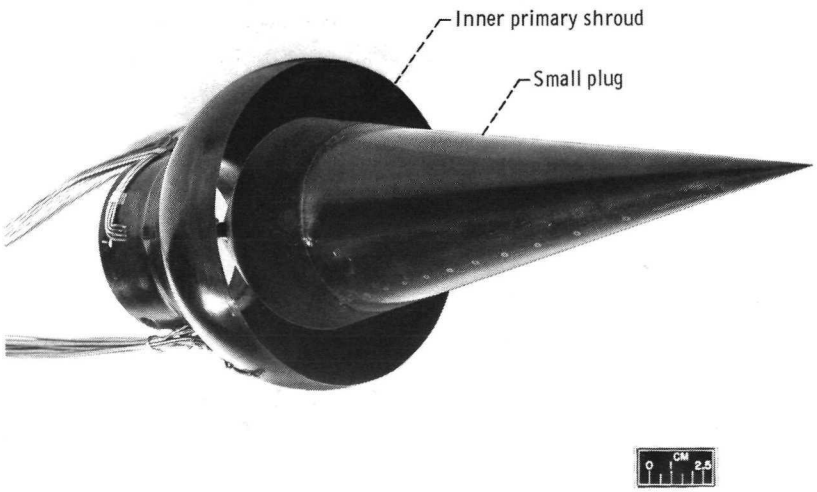

(b) Small plug assembled inside inner primary shroud.

C-72-3299

Figure 6. - Test models.

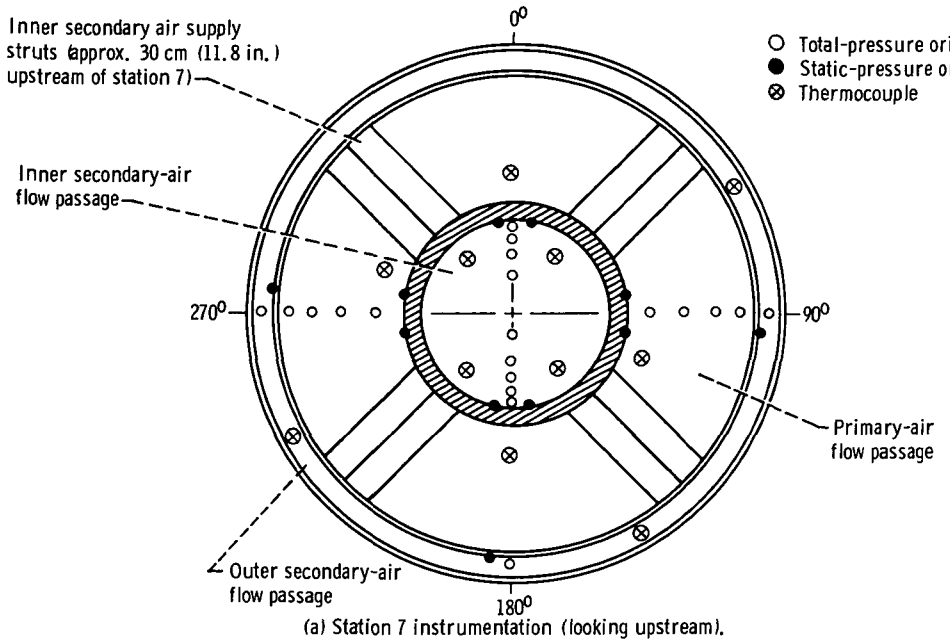

(a) Station 7 instrumentation (looking upstream).

Shroud static-pressure locations

Orifice	X/d_m
1	-0.478
2	-.188
3	.083
4	.318
5	.553
6	.789
7	-.366
8	-.274
9	-.187
10	-.076
11	-.057
12	-.037
13	-.023
14	-.007

Plug static-pressure locations

Orifice	Small plug X/d_m	Large plug X/d_m
15	-0.389	-0.416
16	-.301	-.320
17	-.211	-.211
18	-.134	-.133
19	-.054	-.039
20	-.018	.006
21	.026	.065
22	.073	.127
23	.121	.191
24	.170	.259
25	.223	.331
26	.277	.406
27	.336	.484
28	.400	.569
29	.467	.661
30	.542	.761
31	.623	.874
32	.720	1.004
33	.837	1.163
34	1.010	1.395

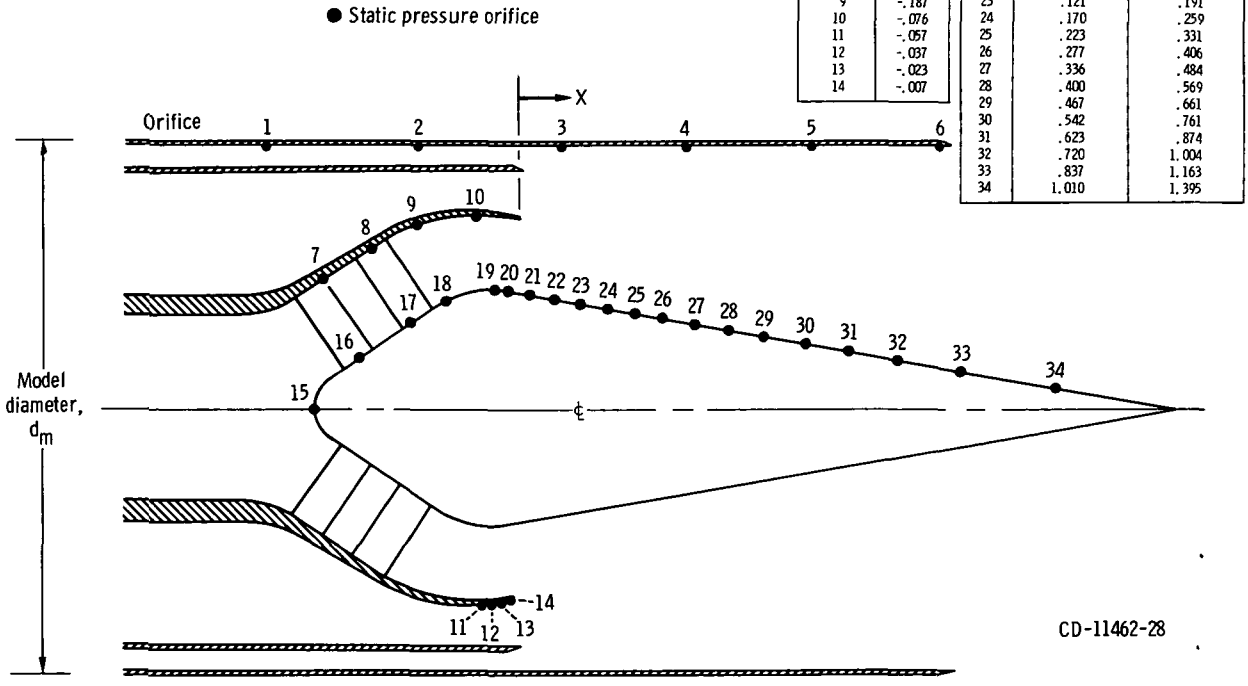

(b) Nozzle static-pressure instrumentation.

Figure 7. - Model instrumentation. (All dimensions are in cm (in.).)

Note: All total pressures are located on the centroids of equal areas.

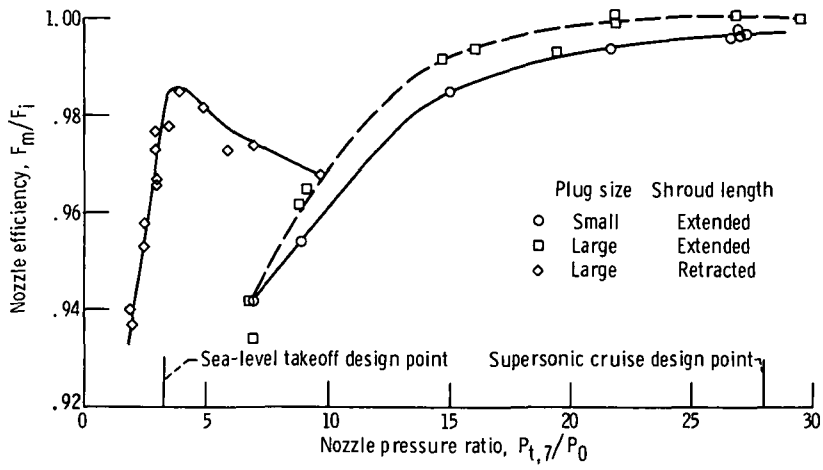

Figure 8. - Effect of shroud length and plug size on measured nozzle thrust efficiency. Inner secondary weight flow ratio, 0.05; outer secondary weight flow ratio, 0.03.

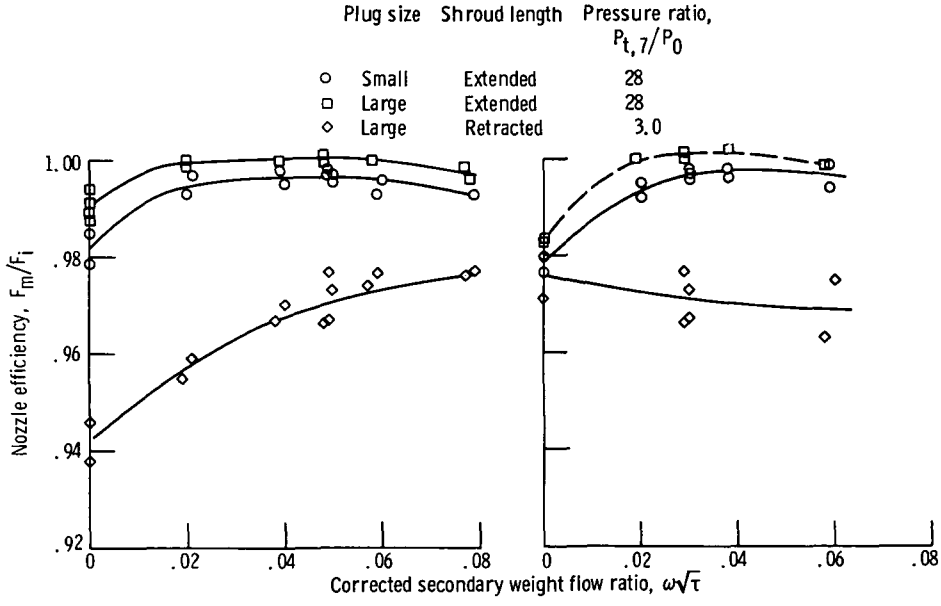

(a) Inner secondary. Outer secondary weight flow ratio held constant at 0.03.

(b) Outer secondary. Inner secondary weight flow ratio held constant at 0.05.

Figure 9. - Effect of secondary weight flow on measured nozzle thrust efficiency.

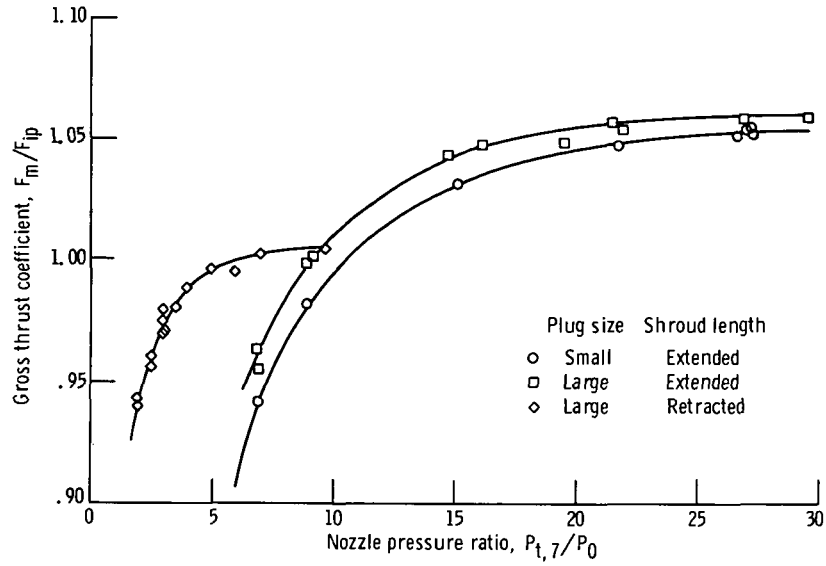

Figure 10. - Effect of shroud length and plug size on nozzle gross thrust coefficient. Inner secondary weight flow ratio, 0.05; outer secondary weight flow ratio, 0.03.

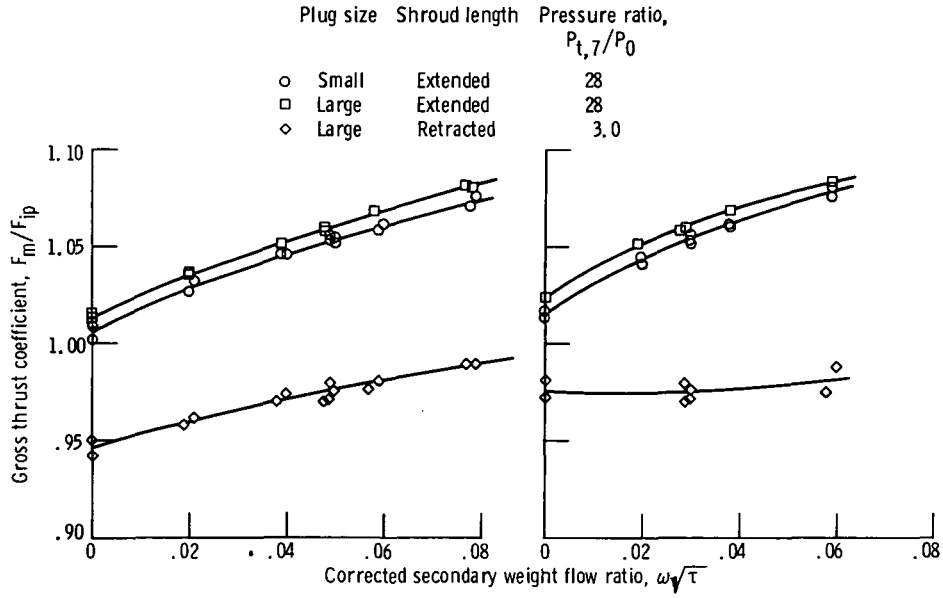

(a) Inner secondary. Outer secondary weight flow ratio held constant at 0.08.

(b) Outer secondary. Inner secondary weight flow held constant at 0.05.

Figure 11. - Effect of secondary weight flow on nozzle gross thrust coefficient.

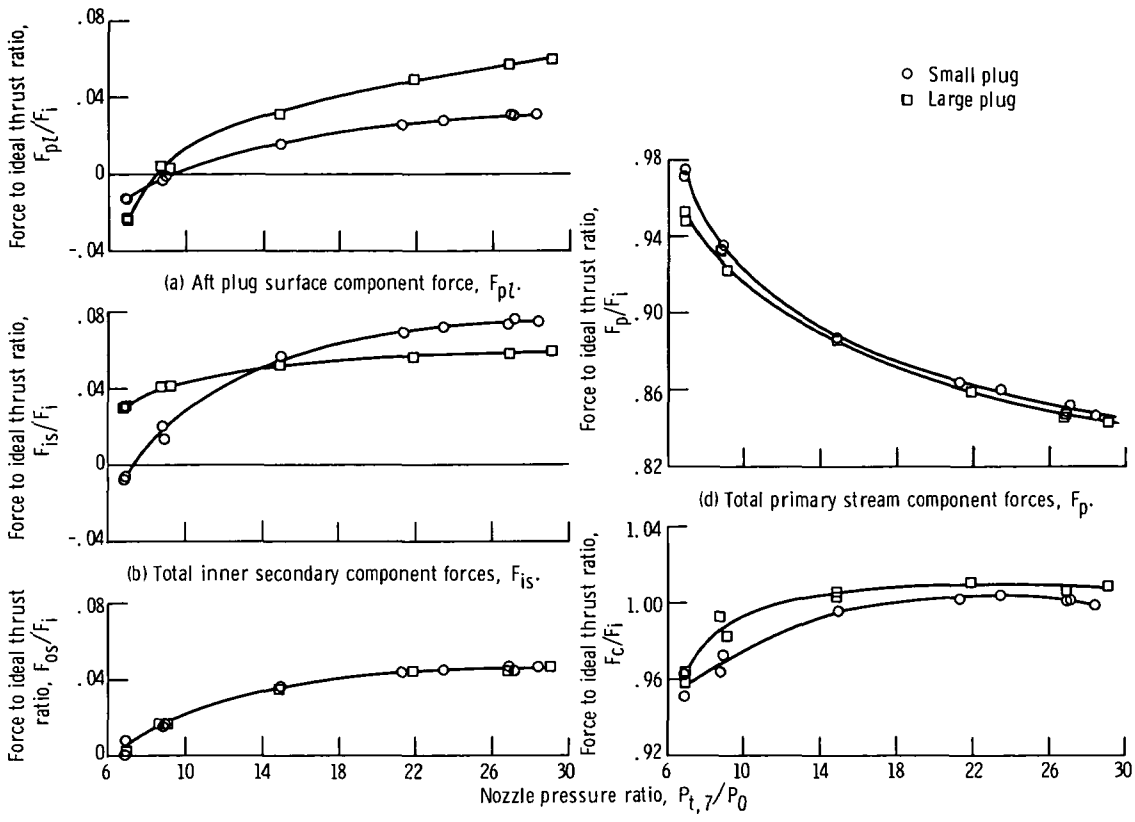

Figure 12. - Effect of plug size on component forces. Extended shroud; inner secondary weight flow ratio, 0.05; outer secondary weight flow ratio, 0.03.

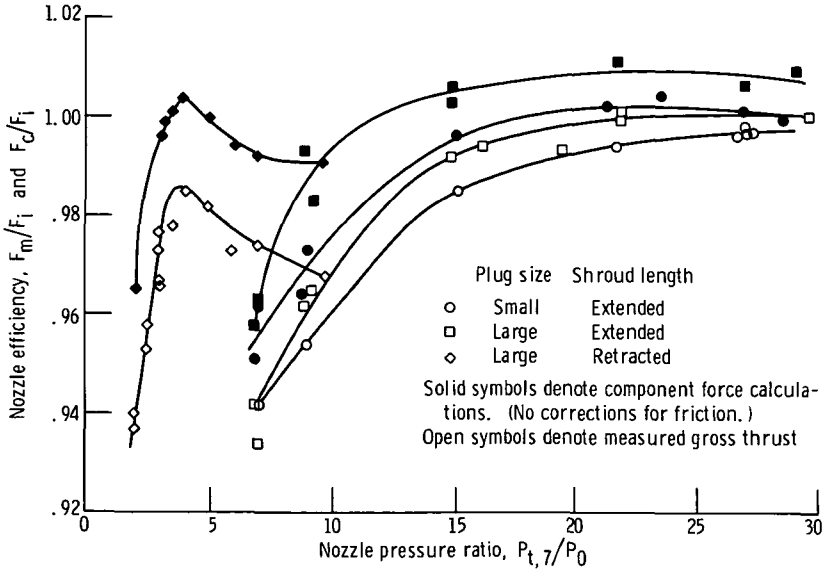

Figure 13. - Comparison of nozzle efficiency based on component forces with measured nozzle efficiency. Inner secondary weight flow ratio, 0.05; outer secondary weight flow ratio, 0.03.

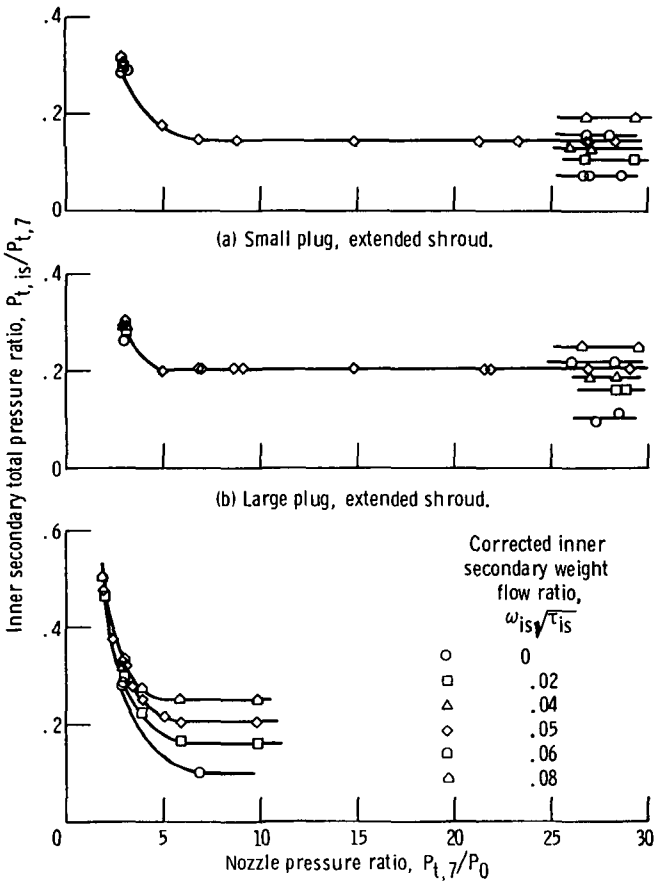

Figure 14. - Pumping characteristics of inner secondary flow passage. Outer secondary weight flow ratio, 0.03.

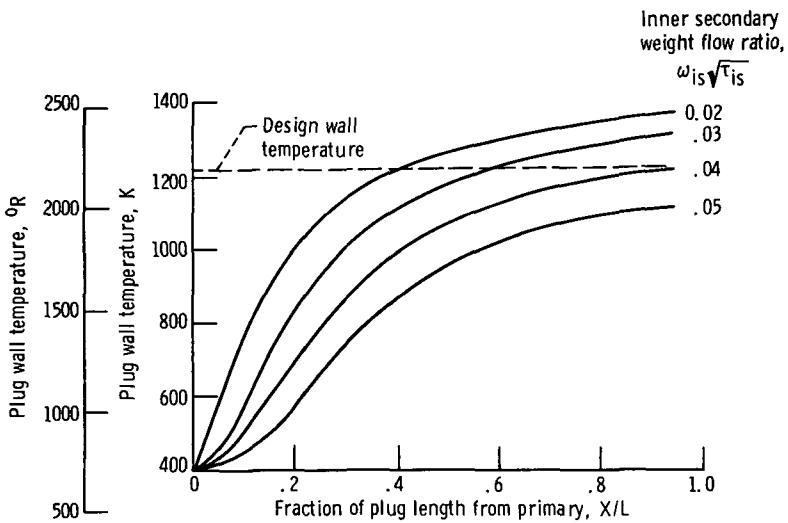

Figure 15. - Calculated plug wall temperatures for several cooling flow rates for 63.5-centimeter (25 in.) outer shroud diameter ram-air-cooled plug nozzle at sea-level takeoff conditions with maximum afterburning. Film cooling correlation, Hatch-Papell; hot gas temperature, 1944 K (3500° R); plug diameter (small), 33.02 centimeters (13 in.); inner secondary slot height, 5.97 centimeters (2.35 in.); nozzle pressure ratio, 2.8.

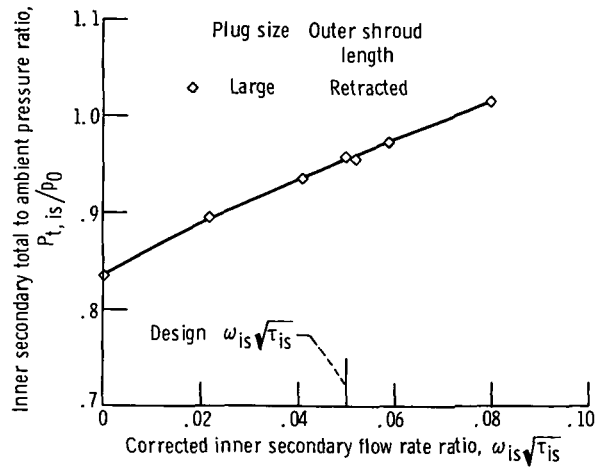

Figure 16. - Inner secondary flow pressure recovery requirements. Outer secondary weight flow ratio, 0.03; nozzle pressure ratio, 3.0.

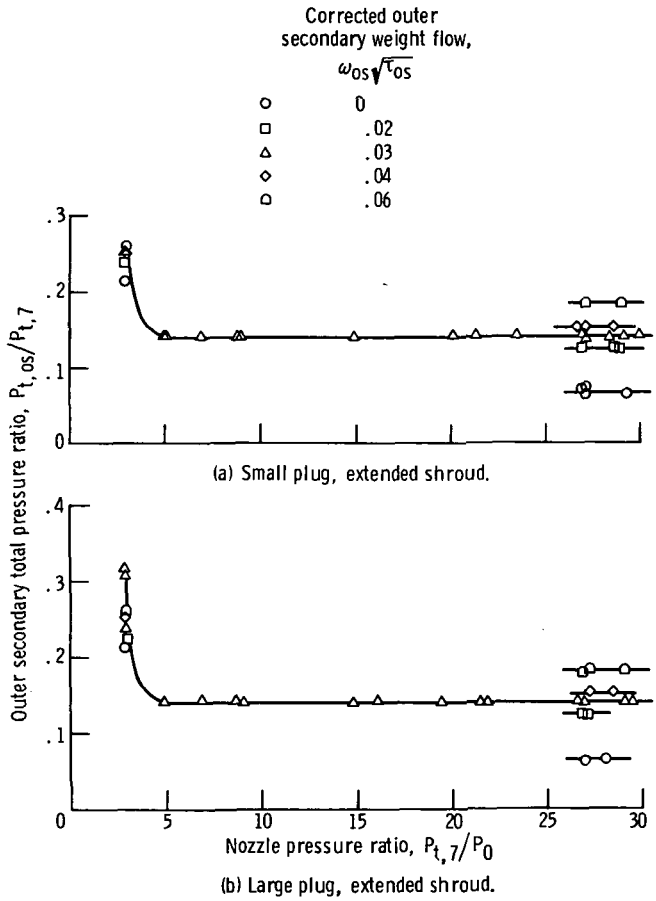

Figure 17. - Pumping characteristics of outer secondary flow passage. Inner secondary weight flow ratio, 0.05.

NASA-Langley, 1973 —— 28

NATIONAL AERONAUTICS AND SPACE ADMINISTRATION
WASHINGTON, D.C. 20546

OFFICIAL BUSINESS
PENALTY FOR PRIVATE U. E $300

SPECIAL FOURTH-CLASS RATE
BOOK

POSTAGE AND FEES PAID
NATIONAL AERONAUTICS AND
SPACE ADMINISTRATION
451

U.S.MAIL

POSTMASTER: If Undeliverable (Section 158 Postal Manual) Do Not Return

"The aeronautical and space activities of the United States shall be conducted so as to contribute . . . to the expansion of human knowledge of phenomena in the atmosphere and space. The Administration shall provide for the widest practicable and appropriate dissemination of information concerning its activities and the results thereof."

—NATIONAL AERONAUTICS AND SPACE ACT OF 1958

NASA SCIENTIFIC AND TECHNICAL PUBLICATIONS

TECHNICAL REPORTS: Scientific and technical information considered important, complete, and a lasting contribution to existing knowledge.

TECHNICAL NOTES: Information less broad in scope but nevertheless of importance as a contribution to existing knowledge.

TECHNICAL MEMORANDUMS: Information receiving limited distribution because of preliminary data, security classification, or other reasons. Also includes conference proceedings with either limited or unlimited distribution.

CONTRACTOR REPORTS: Scientific and technical information generated under a NASA contract or grant and considered an important contribution to existing knowledge.

TECHNICAL TRANSLATIONS: Information published in a foreign language considered to merit NASA distribution in English.

SPECIAL PUBLICATIONS: Information derived from or of value to NASA activities. Publications include final reports of major projects, monographs, data compilations, handbooks, sourcebooks, and special bibliographies.

TECHNOLOGY UTILIZATION PUBLICATIONS: Information on technology used by NASA that may be of particular interest in commercial and other non-aerospace applications. Publications include Tech Briefs, Technology Utilization Reports and Technology Surveys.

Details on the availability of these publications may be obtained from:

SCIENTIFIC AND TECHNICAL INFORMATION OFFICE

NATIONAL AERONAUTICS AND SPACE ADMINISTRATION

Washington, D.C. 20546